JOURNAL OF GUIDANCE, CONTROL, AND DYNAMICS
Vol. 15, No. 4, July-August 1992

Minimizing Spacecraft Attitude Disturbances in Space Manipulator Systems

Miguel A. Torres* and Steven Dubowsky†
Massachusetts Institute of Technology, Cambridge, Massachusetts 02139

This paper presents a technique called the enhanced disturbance map to plan space manipulator motions that will result in relatively low spacecraft disturbances. This subject is of significant concern because future robotic systems used in space may encounter problems due to the dynamic disturbances imposed on their spacecraft by their manipulator motions. Although a spacecraft's attitude control reaction jets can compensate for these dynamic disturbances, jet fuel is a limited resource and excessive disturbances would limit the life of a system. The enhanced disturbance map can aid in understanding this complex problem and in the development of algorithms to reduce disturbances, including ones that use manipulator redundancy to eliminate the disturbances.

Introduction

A NUMBER of telerobotic manipulator systems have been proposed as alternatives to costly and hazardous extra vehicular activity (EVA) in future space missions.[1] However, the development of such robotic systems creates a number of technical challenges, including those in the dynamics and controls area.[2] To solve some of these dynamics and controls problems, a number of planning, control, and modeling algorithms have been proposed in recent years for such systems.[3-18] These include algorithms for time-optimal manipulator motions that would prevent attitude control system reaction jet saturation, and control algorithms that use endpoint sensing.[5,10-12] Studies have also proposed simplified dynamic models of free-floating space manipulator systems in order to reduce the computational effort required for their control.[14] Finally, some fundamental limitations of free-floating space manipulators, including dynamic singularities, have also been found.[15]

Many of the problems in the control of space manipulators result from the dynamic disturbances to the spacecraft attitude and position caused by manipulator motions. If the resulting spacecraft motions are not controlled, such as in free-floating systems, then the system performance could be degraded seriously. Although these spacecraft motions can be controlled using the system's attitude control reaction jets, this could require substantial amounts of attitude control fuel, limiting the useful on-orbit life of the system.[16] To minimize the dynamic disturbances acting on the spacecraft and, hence, enhance a system's life, planning algorithms employing numerical optimization techniques have been proposed.[17,19] Unfortunately, these techniques, like most numerical optimizations of highly nonlinear problems, can require excessive amounts of computational effort for realistic systems and cannot guarantee global optimal solutions.[17,18] They also fail to provide insights into the structure of the problem that can aid the system planner in finding the best solution.

A virtual manipulator (VM) method has been used to study the dynamic coupling between a space manipulator and its spacecraft.[6-9] The VM simplifies the modeling of this coupling and has been used to develop a tool called the disturbance map (DM).[7,9] The DM improves the understanding of the dynamic disturbance problem by graphically showing directions of the manipulator's motion in joint space that result in maximum and minimum dynamic disturbances to the spacecraft.

It was suggested that the DM could be used for planning the paths of manipulators so as to reduce manipulator motion-caused dynamic disturbances to its spacecraft attitude. However, in its original form, the DM was not an effective tool for this purpose. The fixed-attitude restricted Jacobian or the FAR-Jacobian has also been proposed as a method to find manipulator paths that result in reduced-attitude disturbances to a free-floating spacecraft.[13]

This paper presents an improved form of the DM called the enhanced disturbance map (EDM) and shows how it can be effectively used to plan manipulator motion to reduce these disturbances. Reducing manipulator-caused disturbances reduces the need for a space manipulator system to carry large amounts of costly attitude fuel. The paths found using the EDM can be used either directly or as good starting solutions for numerical optimization methods to decrease computational effort and increase the likelihood that such solutions will converge to the globally optimal ones.

An additional method is presented for efficiently calculating the EDM of manipulators with more than two degrees of freedom. The original DM was applied only to simple two-link planar manipulator systems.

Three methods that use the EDM are proposed to suggest paths for a given manipulator that result in low-attitude fuel consumption. The first uses the EDM to position and orient a spacecraft so that a zero dynamic disturbance path can be found between given endpoint positions in inertial space. The second selects reduced disturbance paths by avoiding regions in a manipulator's joint space where small manipulator motions cause large disturbances to the spacecraft. This method is termed the hot spot approach. Finally, the third method uses the EDM to find zero disturbance paths for redundant manipulators.

System Dynamic Model

Consider a system with an n-degree-of-freedom (DOF) rigid manipulator mounted on a rigid spacecraft. The six-DOF spacecraft requires three positions and three orientations in inertial space. The six coordinates are the inertial position of its centroid expressed in body-fixed axes $X_b = [x,y,z]^T$ and its orientation in terms of roll, pitch, and yaw angles expressed also in body-fixed axes $\Theta_b(\phi,\theta,\psi)$; see Fig. 1.

A set of n coordinates is required to describe the configuration of the n-DOF manipulator. These coordinates are chosen to be the relative displacements of the manipulator's joints $q = [q_1,q_2,\ldots,q_n]^T$; see Fig. 1. The generalized coordi-

Received March 13, 1991; revision received Nov. 18, 1991; accepted for publication Dec. 17, 1991.

*Graduate Student, Department of Mechanical Engineering.
†Professor, Department of Mechanical Engineering.

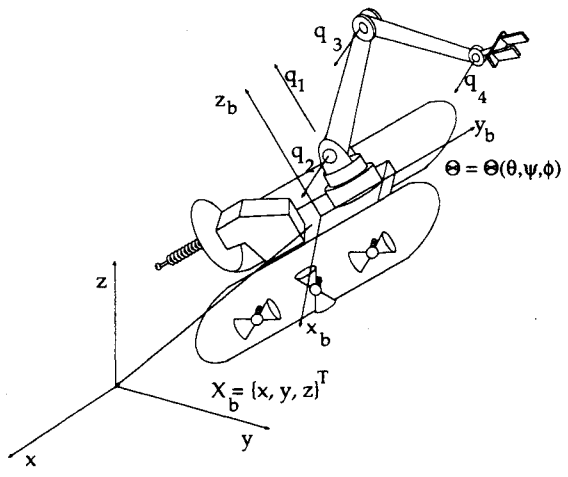

Fig. 1 System generalized coordinates.

nates used to write the dynamics of the system are chosen as the position of the spacecraft expressed in the body-fixed frame X_b, the orientation of the spacecraft Θ_b described earlier (note that Θ_b represents finite rotations that are compounded according to the laws of matrix multiplication not vector addition[22]), and the manipulator's joint angles q. These variables are used to form the generalized coordinates ξ, where $\xi(X_b, \Theta_b, q)$. $\dot{\xi}$ is a generalized velocity vector defined as $\dot{\xi} = [\dot{X}_b, \dot{\Theta}_b, \dot{q}]^T$.

To model the effect of the spacecraft's reaction jets, a generalized force vector is defined as $F = [f_x, f_\theta, f_q]^T$, where $f_x \in \Re^3$ and $f_\theta \in \Re^3$ are external forces and torques produced by the jets expressed in the body-fixed frame and acting on the centroid of the spacecraft. The elements of the vector $f_q \in \Re^n$ are the torques produced by the n manipulator joint actuators.

Based on this set of generalized coordinates, the equation of motion for the system can be written as

$$H(\xi)\ddot{\xi} + C(\xi,\dot{\xi})\dot{\xi} = F \tag{1}$$

where $H(\xi) \in \Re^{n+6, n+6}$ is the symmetric, positive definite inertia matrix; $C(\xi,\dot{\xi})\dot{\xi} \in \Re^{n+6}$ the Coriolis and centrifugal effects vector; and $F \in \Re^{n+6}$ a generalized force vector.

The generalized momentum vector for the system $\pi \in \Re^{n+6}$ can be written as

$$H(\xi)\dot{\xi} = \pi \tag{2}$$

where

$$\pi = [\pi_x, \pi_y, \pi_z, \pi_\phi, \pi_\theta, \pi_\psi, \pi_1, \pi_2, \ldots, \pi_n,]^T \tag{3}$$

The elements π_x, π_y, and π_z are the x, y, z components of the linear momentum of the center of mass of the spacecraft, and π_ϕ, π_θ, and π_ψ are the components of the angular momentum of the spacecraft. All are measured with respect to the spacecraft body-fixed axes. The components $\pi_1, \pi_2, \ldots,$ and π_n represent the momentum in the direction of each of the manipulator's respective joint axes.

Equation (2) is used to develop an algorithm for computing the disturbance maps. Equation (1) is the basis of a computer simulation using a modified version of the well-known recursive dynamics algorithms of Luh et al.[19,20] and Walker and Orin.[21] The simulation models the dynamic performance of space manipulators, including their spacecraft and control systems.[16] It is used in this study to evaluate the effectiveness of the disturbance map-based planning algorithms.

Disturbance Map

Original Formulation

Infinitesimal changes in spacecraft attitude $\delta\Theta$ can be expressed as a function of infinitesimal manipulator joint motions δq as $\delta\Theta = G'(q,\Theta)\delta q$, where G' is a $3 \times n$ disturbance sensitivity matrix.[7,9] If the spacecraft's angular motions are measured with respect to the spacecraft's body-fixed axes described earlier, then G' becomes G, which is only a function of the joint variable vector q or

$$\delta\Theta_b = G(q)\delta q \tag{4}$$

The vector $\delta\Theta_b$ is defined as the instantaneous rotational disturbance. A singular value decomposition of the matrix G gives the directions and magnitudes of the maximum and minimum spacecraft disturbances as a function of the vector q.[21] References 7 and 9 show that for a two-link planar manipulator, the directions of the minimum and the maximum disturbances are orthogonal in joint space and that the magnitude of the minimum disturbance is zero at all points in this space. Plotting these maximum disturbance directions and the directions of the minimum disturbances at a finite number of points in the two-dimensional joint space results in the original form of the DM, shown in Fig. 2.

At each point $q = [q_1, q_2]^T$ in this map, the magnitude of the maximum disturbance is represented by the length of the arrow. The DM is only dependent on the dynamic and kinematic parameters of the system, i.e., the body masses, inertia tensors, and dimensions. The inertial position and orientation of the spacecraft does not affect the DM's shape if Θ_b is measured with respect to the spacecraft. This makes the DM a suitable tool for visualizing the dynamic behavior of space manipulators based exclusively on their dynamic and kinematics parameters. However, this form makes it difficult to visualize low-disturbance paths, and it is impractical to apply to manipulators with more than two links. An effort to improve these aspects of the DM led to the development of the more effective form of the map discussed in this paper.

Computing the Disturbance Map

References 7 and 9 present the original method for computing the disturbance map for a two-DOF manipulator by using the virtual manipulator. This paper presents a method for efficiently computing the map for manipulators with more than two DOF. Equation (2) defines a generalized momentum vector π based on the selected generalized coordinates described earlier. The inertia tensor of Eq. (1) can be written as[16]:

$$H(\xi) = \begin{bmatrix} A & B \\ C & D \end{bmatrix} \tag{5}$$

where A is a 6×6 symmetric submatrix relating the linear and angular velocity vectors of the spacecraft ($\dot{X}_b^T$ and $\dot{\Theta}_b^T$) to its linear and angular momentum. The $6 \times n$ mass matrix B relates the motion of the joints to the spacecraft's linear and angular momentum, and the matrix C equals B^T. The D is an

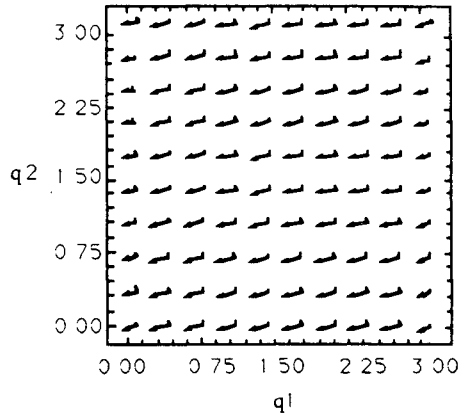

Fig. 2 Origin disturbance map for a two-link planar space manipulator.

$n \times n$ matrix relating the joint velocities to their momenta. It is not used in calculating the EDM. Note that the vector components of $\dot{\Theta}_b$ are defined as $d\phi/dt$, $d\theta/dt$, and $d\psi/dt$.

At this point, it is assumed that the system is at rest and no external forces of torques act on it during the maneuver. This assumption is violated when reduction jets are used to control the spacecraft's position and attitude. Hence, the analysis presented below yields an approximation of directions in joint space of the minimum and maximum disturbance to the spacecraft. A more detailed discussion of the validity of this approach is presented later in this paper.

With the system initially at rest, Eq. (2) becomes

$$H(\xi)\dot{\xi} = 0 \tag{6}$$

Using Eq. (5) and recalling that ξ is $[X_b, \Theta_b, q]^T$, Eq. (6) is rewritten as

$$A[\dot{X}_b^T, \dot{\Theta}_b^T]^T + B\dot{q} = 0 \tag{7}$$

Solving for the vector $[\dot{X}_b^T, \dot{\Theta}_b^T]^T$ yields

$$[\dot{X}_b^T, \dot{\Theta}_b^T]^T = -A^{-1}B\dot{q} \tag{8}$$

By replacing the derivative operation by a variation, letting $Z = [Z_1, Z_2]^T = -A^{-1}B$, and noting the Z_1 and Z_2 are $3 \times n$ matrices, Eq. (6) becomes

$$\begin{bmatrix} \delta X_b \\ \delta \Theta_b \end{bmatrix} = \begin{bmatrix} Z_1 \\ Z_2 \end{bmatrix} \delta q \tag{9}$$

The goal of the algorithm is to find the relationship between changes in the orientation of the base $\delta\Theta_b$ and the motion of the manipulator joints δq. This relationship is obtained from Eq. (9) as

$$\delta\Theta_b = Z_2 \delta q \tag{10}$$

Equation (10) is the same as Eq. (4) required for the DM, and so G is Z_2. The matrix Z_2 is a submatrix of $H(\xi)$, which is computed quite efficiently by the modified Walker and Orin algorithm, modified in this study to treat manipulators with moving bases.[16] Finally, a singular value decomposition of the matrix Z_2 gives the directions and magnitudes of maximum and minimum disturbances required for plotting the DM.[21]

Enhanced Disturbance Map

The EDM derives from studying the attitude disturbances to a system's spacecraft by its manipulator at an arbitrary point in the manipulator's joint space. Consider the disturbance for a two-DOF manipulator at some point in its joint space, such as shown in Fig. 3a. References 7 and 9 show that for all such points there are directions of maximum and minimum disturbances and moreover that these directions are perpendicular to each other. The magnitude of the disturbance varies in a dipole fashion as shown in Fig. 3a.[16] The dipole shape shows how the magnitude of the disturbance $|\delta\Theta_b|$ varies as a function of the angle α, shown in Fig. 3a. The disturbance is a maximum at

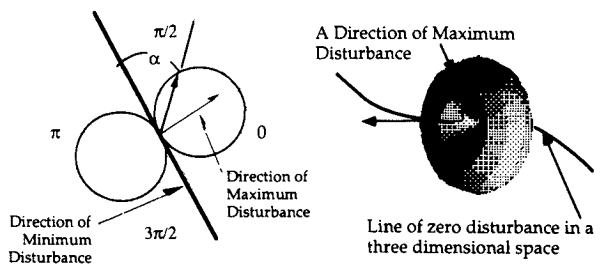

a) Two-link manipulator **b) Three-link manipulator**

Fig. 3 Disturbance magnitude for a point in the disturbance map.

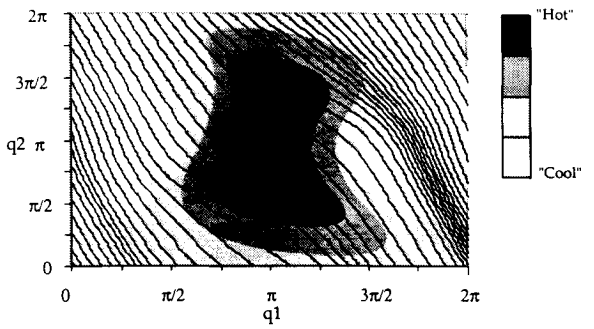

Fig. 4 The enhanced disturbance map.

$\alpha = 90$ deg and a minimum of zero along a line of zero disturbance, when $\alpha = 0$.

The disturbance characteristics of the three-link spatial manipulator with two parallel axes, such as shown in Fig. 1, are presented in Fig. 3b. These results reveal that, as in the case with the two-DOF manipulator, there exists a direction in joint space for which small manipulator motions do not disturb the spacecraft attitude.

There may be more than one direction of zero disturbance motion, such as in a redundant system. The dimension of the subspace of joint space $\Re_{zero}$ in which manipulator motions produce no vehicle disturbances can be found by examining the rank of matrix Z_2. The dimension of this subspace is given by

$$\Re_{zero} = \dim[N(Z_2)] \tag{11}$$

where N denotes the kernel or null space[21] of Z_2.

The existence of these local zero disturbance directions suggests that paths constructed to lie largely along the lines of zero disturbance will result in low fuel usage. Motions across or perpendicular to a zero disturbance line will result in a local maximum spacecraft disturbance, or high fuel consumption. The original DM was recast to show the lines of zero disturbance, such as shown in Fig. 4. This new form is called the EDM; it permits the representation of three-DOF manipulators on a graphics computer workstation. The magnitudes of the maximum disturbance are shown by coloring the lines proportionally to the maximum disturbance magnitude at that point. This coloring makes obvious high and low maximum disturbance areas, called hot spots and cool spots, respectivley. Manipulator motions that cross the lines in a red area, or hot spot, will result in large disturbances of the vehicle. Manipulator motions that cross the lines in cool areas will result in smaller disturbances. These observations play an important role in the development of the path-planning strategies discussed in the following. Unfortunately, it is not possible to reproduce the colors in the figures of this paper and, therefore, where needed, they are represented by background shading.

Attitude Disturbances, Fuel Consumption, and the Enhanced Disturbance Map

The spacecraft of future space manipulator systems are likely to be equipped with reaction jets, reaction wheels, or both. Reaction jets can control both the attitude and the position of the system. However, the amount of fuel that can be carried to power these systems is limited. Reaction wheels, which can be powered by solar energy, can only control a system's attitude and can be easily saturated by large rotational disturbances. As discussed later, space manipulator systems using either or both of these spacecraft control techniques can benefit from the use of the EDM in planning the motions of their manipulators.

The amount of instantaneous power required from a system's reaction wheels to compensate for the rotational disturbances produced by its manipulator's motion can be shown to

be directly proportional to the instantaneous rotational disturbance $\delta\Theta_b$ given by Eq. (4) and plotted in the disturbance maps.[9,16] So, for example, systems with manipulators whose paths follow zero disturbance lines in the EDM would avoid reaction wheel saturation problems. Determining the amount of reaction jet fuel required to correct a spacecraft's position and attitude in the presence of manipulator motion disturbances is not as simple. It can be shown that the fuel used to hold a spacecraft stationary during a manipulator's maneuver varies directly as the level of dynamic disturbance to the spacecraft.[16] These disturbances are a function of the path taken by the manipulator and the velocity of the manipulator's motion along that path. Generally, the faster the motion, the greater the fuel usage. This study does not consider the issue of the dependence of fuel usage on manipulator speed because we assume that if a manipulator path is found that results in relatively low disturbance to the spacecraft, then relatively low fuel usage results. These low-disturbance paths can be used directly in cases where the manipulator velocity profile is determined by other considerations, or as initial paths for numerical optimization procedures that include the effects of manipulator speed.

Disturbance to the spacecraft consists of translational and rotational components. Reaction jets would need to compensate for the translational component if translations of the spacecraft are undesirable. Rotational disturbance must be overcome to eliminate spacecraft attitude changes. The total rotational disturbance is defined to be the integral of the absolute value of the instantaneous dynamic disturbances $|\delta\Theta_b|$ along the manipulator path.[16] The fuel consumption due to linear disturbances has been shown in simulations, at least for the systems considered in this system, to be smaller than that due to the rotational disturbance. If the translational disturbance is uncontrolled during a manipulator motion between given endpoints, it can also be shown that the total translational shift of the spacecraft is not a function of the manipulator's path between those points.[8] Hence, we assume that the fuel required to hold the linear location of the system stationary is not a strong function of the manipulator paths for relatively smooth paths. Therefore, this study focuses on developing methods that would minimize both the instantaneous rotational disturbance to the spacecraft to prevent saturation of reaction wheels and the total rotational disturbance to minimize reaction jet fuel usage.

Recall that EDM is developed based on the following assumptions: 1) That the mass properties of the manipulator's links and the spacecraft are constant, and 2) that the generalized momentum π, i.e., $d\pi/dt$ of the system, is constant and equal to zero with respect to some Newtonian frame of reference.

These assumptions will be violated if the manipulator grasps an object. Such an action may require that the EDM be recalculated. Then the assumption of zero generalized momentum will not be valid if the system is experiencing a linear acceleration or it is tumbling. However, a manipulator system would not be expected to perform tasks while it is tumbling or while its center of mass is experiencing a substantial change in linear velocity.

The use of reaction jets will violate the assumption of constant generalized momentum. Reaction jets will change the shape of the EDM. Clearly, as the forces and torques produced by reaction jets approach zero, the instantaneous directions of minimum and maximum disturbance will converge to those predicted by the EDM as computed earlier. Hence, low-disturbance paths will result in low-reaction jet forces and torques, which result in an instantaneous EDM shape closer to the computed zero momentum EDM. The approximation will not be valid for paths that result in high disturbances. This has been our experience with the techniques and of the examples presented in this paper.

Table 1 Dynamic characteristic for the two-link system

	Mass, kg	S, m	L, m	I, kg-m-m
Base	500.0	0.0	n/a	30.0
Link 1	10.0	0.0	5.0	3.0
Link 2	10.0	5.0	5.0	5.0

Techniques for Minimizing Fuel

Three methods are discussed for using the EDM to suggest paths that result in less attitude fuel consumption. First, the EDM is used to position and orient the spacecraft so that a zero dynamic disturbance path can be found. This approach will be seen to be most effective in repetitive manipulator motions. Second, paths are selected that avoid regions where small motions of the manipulator cause large disturbances to the spacecraft. Finally, the EDM is used to find zero disturbance paths for redundant manipulators. The simple system shown in Fig. 5 is used in the first two examples presented. The system's parameters are given in Table 1.

Spacecraft Relocation

It is always possible, given the initial and final endpoints of a motion in inertial space, to relocate the spacecraft position and orientation for planar systems so that a manipulator path exists that results in zero angular spacecraft disturbance.[16] Such a path will be achieved if the initial and final positions of the manipulator lie on the same zero disturbance line in the EDM, and if the manipulator follows that zero disturbance line from the initial point to the final position. Although fuel must be spent during the initial relocation of the spacecraft, little or no fuel will be spent in the actual manipulator maneuver. Hence, such a strategy would be most appropriate for cases where the manipulator needs to make a series of nearly repetitive moves within an area fixed in inertial space. Algorithms to find such paths can be developed by noting that the initial and final EDM positions of the manipulator for given inertial end-effector positions depend on the position and orientation of the spacecraft. One such algorithm developed here first finds the EDM position for a system when its manipulator's end effector is at its desired initial position in inertial space and its spacecraft is at some arbitrary position and orientation, see Fig. 6a. Figure 6b shows the initial position of the manipulator on the disturbance map, called point I. Then the zero disturbance line that passes through point I is computed,

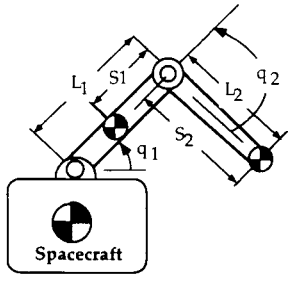

Fig. 5 Two-link system.

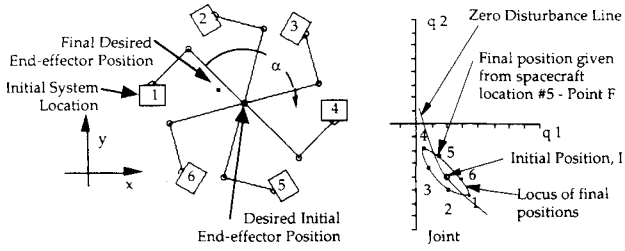

a) Inertial space b) Joint space

Fig. 6 Effect of an imagined spacecraft rotation about its manipulator initial end-effector location.

see Fig. 6b. Next, imagine the system is rotated about this initial end-effector position in inertial space by an angle α, such as is shown in Fig. 6a. Note that the system EDM would not change for such a system rotation because the EDM shows the disturbances with respect to the spacecraft axes. However, such a rotation would change the EDM position of the manipulator's final inertial path point position without changing the EDM position of the initial path point. Figure 6b shows that the locus of final positions of the manipulator system were rotated around the initial position. The algorithm determines the rotation angle required for the final EDM position, called F in Fig. 6b, to be on the same zero disturbance line that passes through the initial position. A complete description of this algorithm is contained in Ref. 16.

In the following example, the objective is to move the manipulator endpoint, shown in Fig. 7a, from an initial point in inertial space, point I, to a final point, point F. An arbitrary spacecraft location and an arbitrary path from point I to point F are also shown in Fig. 7a. This path is shown in the EDM in Fig. 7c, as the line from I to F, where it runs almost perpendicular to the EDM zero disturbance lines. Simulations show that this path results in the use of substantial reaction jet control fuel to hold the spacecraft completely stationary. However, by using the algorithm described in the preceding example, a new position and orientation of the spacecraft was calculated, see Fig. 7b. This placed the final point, called F′, on the same zero disturbance line as the initial point, see Fig. 7c. Using the zero disturbance line I to F′ as the path, the rotational disturbances are zero; hence the fuel usage is essentially zero.

As stated earlier, this approach is most appropriate for cases where the manipulator will be making a series of nearly repetitive moves because of the reaction jet control fuel required to reposition the spacecraft.

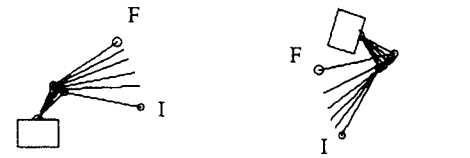

a) Arbitrary path b) Low-disturbance path

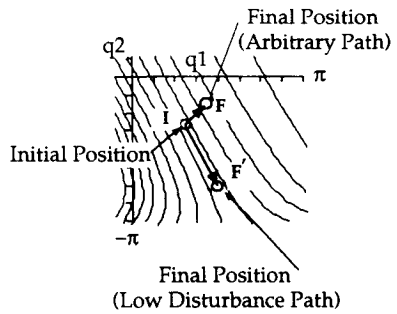

c) Disturbance path

Fig. 7 System—before and after spacecraft relocation.

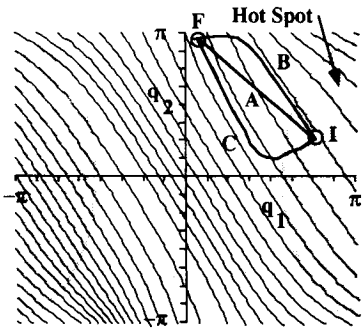

Fig. 8 Path selection using the hot spot approach: A = straight line; B = cool path; C = hot path.

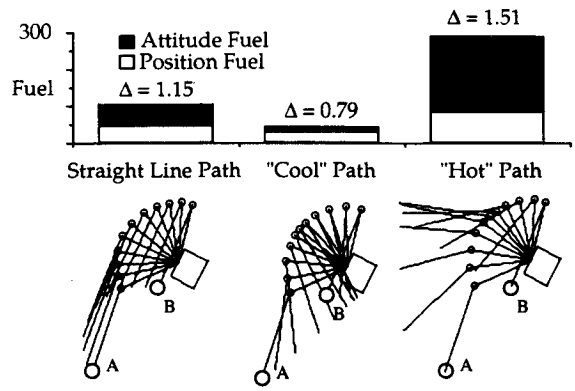

Fig. 9 Amount of spacecraft control fuel required and corresponding inertia motion of the space manipulator for each path.

Hot Spot Method

Another method of minimizing fuel consumption based on the EDM is the hot spot method, which is useful in cases where it is not practical to reposition the spacecraft, including those occasions when interference with other objects may result.

Consider the case where the initial and final manipulator end-effector positions are fixed in inertial space. These points are also fixed in the EDM. We assume that the attitude control system keeps the spacecraft stationary during the manipulator's motion. Figure 8 shows the EDM and its pseudocoloring for the two-link space manipulator shown in Fig. 5. As the manipulator moves its endpoint from initial point to final points in inertial space, its joint angles will move between the corresponding points I and F in the EDM contained in Fig. 8. The dark areas of the EDM, shown in Fig. 8, represent hot spots, or areas of higher maximum dynamic disturbance. Notice that the initial configuration or point I in this example lies in a hot spot. This path would produce substantial rotational disturbances to the spacecraft. Thus, the hot spot approach is the following: If a path must go through EDM regions of large disturbance, then it should follow the zero disturbance lines as closely as possible. When disturbances are low, at cool spots, the path may move across disturbance lines. Clearly this can be done more effectively when the EDM is plotted in color where finer degrees of the maximum disturbance can be seen. Three paths were considered following this rule for the system shown in Fig. 5 in order to show the effectiveness of this approach. These are shown in Fig. 8. The first is the straight line from I to F. The second is contoured to follow the zero disturbance line in the hot region. The third moves across the zero disturbance lines in the hot region.

The total amount of reaction jet control fuel required to hold the spacecraft stationary in each of the three cases was computed using the simulation programs described earlier, and are shown in Fig. 9. Recall that fuel usage is a function of the velocity profile of a manipulator along its path, as well as the shape of the path in the EDM. The same velocity profile was used in each case in this example. The manipulator started from rest at point I and moved with a constant acceleration until midway along the path; it then used the same constant deceleration to come to a stop at its final position at F. All these movements were completed in 1.0 s.

Figure 9 clearly shows that the path selected by the hot spot approach, shown in Fig. 8, reduces the amount of fuel below the level of the simple straight line path; moving across the disturbance lines in high-disturbance regions increases fuel consumption. Figure 9 also shows that the fuel required to compensate for the translational disturbances is less than that required for the rotational disturbances, except in the case where the rotational fuel has been optimized by the EDM. Furthermore, although the amount of position fuel varies from path to path, it is not a strong function of the path used.

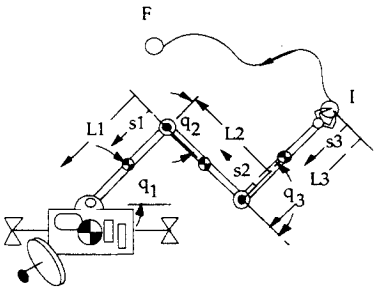

Fig. 10 Redundant three-link planar space manipulator.

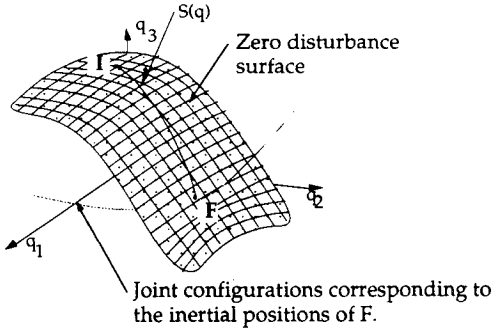

Fig. 11 Zero disturbance manifold of a three-DOF redundant planar manipulator.

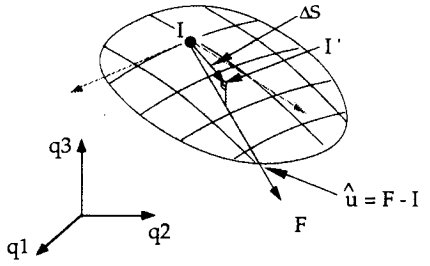

Fig. 12 Method for computing $S(q)$.

A measure of the angular disturbance, called Δ (rad), produced by manipulator motion was computed for each of the paths as the integral over the path of the magnitudes of the disturbance $|\delta\Theta_b|$. The values of Δ for each path are shown in Fig. 9. It can be seen that this simply computed measure agrees well with actual fuel usage.

Minimizing Fuel in Redundant Systems

The EDM has led to an algorithm to reduce fuel consumption in systems with redundant manipulators. Consider the problem of a three-link redundant manipulator moving in a planar space from point I to F, with its spacecraft held stationary by its control system (see Table 2 and Fig. 10).

The form of the EDM for such a three-DOF redundant manipulator is shown in Fig. 11. The EDM will be a three-dimensional space, whose axes are the three manipulator joint variables. For this redundant manipulator, the subspace $\Re_{zero}$ of the directions of zero angular dynamic disturbance motion can be represented as a two-dimensional manifold or surface in joint space rather than as lines, as for nonredundant manipulators.

Given the initial position of the system, called point I in Fig. 11, the zero disturbance surface passing through this point can be found by the direct application of Eq. (10) and singular value decomposition. Next, it is noted that because the manipulator is redundant, the final position of the end-effector in inertial space F maps into a locus of points, a curved line, in joint space, as shown in Fig. 11. If the value of F in joint space is chosen as the intersection of the zero disturbance surface and this locus, and if the path from I to this point is chosen to lie in the zero disturbance surface, then manipulator motion will not result in any angular disturbances to the spacecraft. This path is called $S(q)$ and can be computed in several ways. One is to compute a unit vector $\hat{u}$ from a point I in the direction of the vector $F-I$, where F and I are the position vectors of the points F and I in joint space, respectively. The vector $\hat{u}$ is given by

$$\hat{u} = \frac{F-I}{|F-I|} \tag{12}$$

The projection of $\hat{u}$ onto the plane tangent to the zero disturbance surface at point I locally defines a direct path toward the required final point, see Fig. 12. The surface at I is found easily by using the two perpendicular zero disturbance directional vectors. The path $S(q)$ is then determined by multiplying the $\hat{u}$ vector by an arbitrary small quantity ΔS to find in new point I' on the zero disturbance surface, $S(q)$. The process is repeated until the vector $F-I'=0$. It should be noted that this algorithm works equally well for nonplanar redundant systems.

The following is an example of the results obtained by this method. The computed paths are simulated with the system's attitude control system on, in order to prevent the spacecraft from moving, and the fuel required for each path is computed. Figure 13a shows the manipulator of Fig. 10 at an initial end-effector position I. Its corresponding position in three dimensional joint space is shown in Fig. 14. The zero disturbance surface passing through point I in joint space is also shown in two views in Fig. 14. Figure 14 also shows an arbitrary path from point I to point F; F corresponds to just one of the

Table 2 Redundant system properties

Spacecraft mass = 10.0 kg		
Link 1 mass = 1.0 kg	$L1 = 1.0$ m	$s1 = 0.5$ m
Link 2 mass = 1.0 kg	$L2 = 1.0$ m	$s2 = 0.5$ m
Link 3 mass = 1.0 kg	$L3 = 1.0$ m	$s3 = 0.5$ m

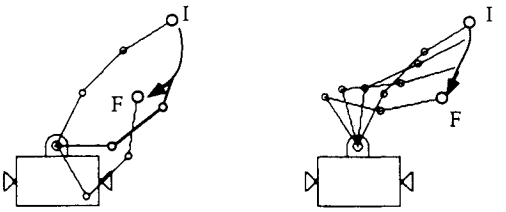

a) Arbitrary path **b) Zero disturbance path**

Fig. 13 Two redundant manipulator paths with the same inertial space endpoints.

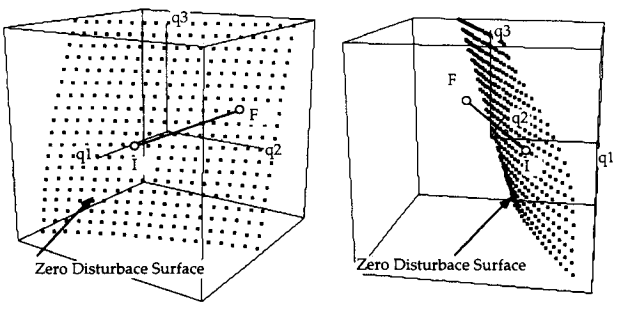

Fig. 14 Redundant space manipulator; arbitrary path.

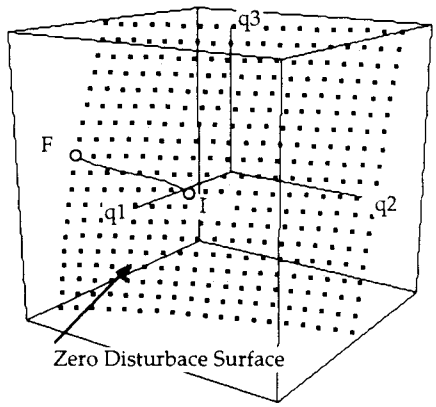

Fig. 15 Redundant space manipulator; computed path maneuver.

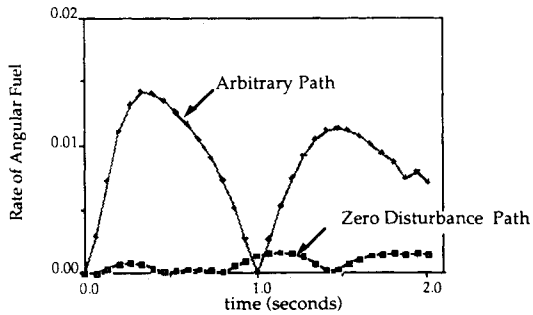

Fig. 16 Rate of fuel consumption (simulation results).

infinite configurations that locate the end-effector at F in inertial space. Notice from the back view in Fig. 14 that this path does not stay on the zero disturbance surface passing through I. Figure 15 shows a path that has been computed to move the manipulator's end-effector from the same points I to F in inertial space while staying on the zero disturbance surface passing through I. This path is shown in Fig. 13b.

The motions along the two paths were simulated allowing reaction jets to compensate for any dynamic disturbance, and the fuel usage was recorded. The velocity profile along the path was chosen to be a half sinusoidal wave with initial and final velocities equal to zero. The magnitudes of the maximum velocity, which varies with the length of the path, were computed so that all maneuvers would take 2 s. Figure 16 shows the rate of fuel consumption to correct for the angular motion of the spacecraft. For the arbitrary path, the total angular and linear fuel required was 0.587 unit of fuel. By contrast, the zero disturbance path required only 0.160 unit, a substantial reduction. This zero disturbance path fuel was required mostly to compensate for translational disturbances to the spacecraft.

In this study, several other algorithms were developed using the EDM to shape manipulator paths to reduce the disturbances to the spacecraft. A description of these methods are beyond the scope of this paper and the reader is referred to Ref. 16.

Conclusions

The enhanced disturbance map has been shown to aid in understanding the problem of dynamic disturbances to spacecraft caused by manipulator motion in space robotic systems and in finding paths to reduce such disturbances. Although the EDM and its zero disturbance lines or surfaces can only be displayed for up to three-DOF manipulators using modern computer graphics terminals, numerical algorithms can be developed that trace their way through the multidimensional joint space of higher-order systems by using the understanding provided by the three-dimensional disturbance maps. For example, this paper shows that the enhanced disturbance map can be used to demonstrate the existence of zero disturbance paths for redundant space manipulators and to develop an algorithm to find such paths. That algorithm is valid for general spatial manipulators with more than six DOF.

The EDM also can be used to obtain good starting solutions for numerical optimization methods that decrease the computational effort for such methods and increase the likelihood that they will converge to true global optimal solutions.

Acknowledgments

The support of this work by NASA Langley Research Center, Automation Branch, under Grant NAG-1-801, and M. Torres' NASA Fellowship is acknowledged.

References

[1]Bronez, M. A., Clarke, M. M., and Quinn, A., "Requirements Development of a Free-Flying Robot—The 'ROBIN'," *Proceedings of the 1986 IEEE International Conference in Robotics and Automation,* IEEE Computer Press Society, Washington, DC, 1986, pp. 667–672.

[2]*Proceedings of NASA Conference on Space Telerobotics,* Pasadena, CA, Jet Propulsion Lab., 1989.

[3]Kohn, W., and Healey, K., "Trajectory Planner for an Autonomous Free-Floating Robot," *Proceedings of the 1986 IEEE International Conference on Robotics and Automation,* IEEE Computer Society Press, Washington, DC, p. 665

[4]Longman, R., Lindberg, R., and Zedd, M., "Satellite-Mounted Robot Manipulators—New Kinematics and Reaction Moment Compensation," *International Journal of Robotics Research,* Vol. 6, No. 3, 1987, pp. 87–103.

[5]Dubowsky, S., Vance, E. E., and Torres, M. A., "The Control of Space Manipulators Subject to Spacecraft Attitude Control Saturation Limits," *Proceedings of NASA Conference on Space Telerobotics,* Jet Propulsion Lab., Pasadena, CA, Vol. IV, Jan.-Feb. 1989, pp. 409–418.

[6]Vafa, Z., and Dubowsky, S., "A Virtual Manipulator Model for Space Robotic Systems," *Proceedings of NASA Conference on Space Telerobotics,* Jet Propulsion Lab., Pasadena, CA, Vol. 3, Jan. 1987, pp. 335–344.

[7]Vafa, Z., and Dubowsky, S., "On the Dynamics of Manipulators in Space Using the Virtual Manipulator Approach," *Proceedings of the 1987 IEEE International Conference on Robotics and Automation,* IEEE Computer Society Press, Washington, DC, pp. 579–585.

[8]Vafa, Z., and Dubowsky, S., "The Kinematics and Dynamics of Space Manipulators: The Virtual Manipulator Approach," *International Journal of Robotics Research,* Vol. 9, No. 4, 1990, pp. 3–21.

[9]Vafa, Z., and Dubowsky, S., "On the Dynamics of Space Manipulators Using the Virtual Manipulator, with Applications to Path Planning," *Journal of the Astronautical Sciences,* Vol. 37, No. 4, Oct.-Dec. 1990, pp. 441–472.

[10]Alexander, H. L., and Cannon, R. H., "Experiments on the Control of a Satellite Manipulator," *Proceedings of the 1987 American Control Conference,* IEEE, New York, June 1987.

[11]Umetani, Y., and Yoshida, K., "Experimental Study on Two Dimensional Free-Flying Robot Satellite Model," *Proceedings of the NASA Conference on Space Telerobotics,* Jet Propulsion Lab., Pasadena, CA, Vol. V, Jan. 1989, pp. 215–224.

[12]Masutani, Y., Miyazaki, F., and Arimoto, S., "Sensory Feedback Control for Space Manipulators," *Proceedings of the IEEE Conference on Robotics and Automation,* IEEE Computer Society Press, Washington, DC, May 1989, pp. 1346–1351.

[13]Nenchev, D., Yoshida, K., and Umetani, Y., "Analysis, Design and Control of Free-Frying Space Robots Using Fixed-Attitude-Restricted Jacobian Matrix," *Proceedings of the Fifth International Symposium on Robotic Research,* MIT Press, Cambridge, MA, 1990, pp. 251–258.

[14]Yamada, K., and Tsuchiya, K., "Trajectory Planning for a Space Manipulator," *Advances in Astronautical Science,* edited by C. A. Thornton, R. J. Proulx, J. E. Prussing, and F. R. Hoots, Vol. 71, Pt. 2, American Astronautical Society, San Diego, CA, 1989, pp. 1265–1281.

[15]Papadopoulos, E., and Dubowsky, S., *Dynamics and Control of Multibody/Robotic Systems with Space Applications,* edited by S. M. Joshi, L. Silverberg, T. E. Alberts, American Society of Mechanical Engineers, New York, DSC-Vol. 15, 1989, pp. 45–52.

[16]Torres, M., "The Disturbance Map and Minimization of Fuel Consumption During Space Manipulator Maneuvers," M.S. Thesis,

Dept. of Mechanical Engineering, Massachusetts Inst. of Technology, Cambridge, MA, 1989.

[17]de Silva, C. W., Chung, C. L., and Lawrence, C., "Base Reaction Optimization of Robotic Manipulators for Space Applications," *Proceedings of the International Symposium of Robots,* IFS Publications, Kempston, UK, 1988.

[18]Quinn, R. D., Chen, J. L., and Lawrence, C., "Redundant Manipulators for Momentum Compensation in Micro-Gravity Environment," *Proceedings of the AIAA Guidance, Navigation and Control Conference,* AIAA, Washington, DC, 1988, pp. 581–587.

[19]Luh, J. Y. S., Walker, M. W., and Paul, R. P. C., "Online Computational Scheme for Mechanical Manipulators," *Journal of Dynamic Systems, Measurements and Control,* Vol. 102, No. 2, 1980, pp. 69–76.

[20]Crandall, S. H., Karnopp, D. C., Kurtz, E. F., and Pridmore-Brown, D. C., *Dynamics of Mechanical and Electromechanical Systems,* Krieger, Malabar, FL, 1982, pp. 57–61.

[21]Walker, M. W., and Orin, D. E., "Efficient Dynamic Computer Simulation of Robotic Mechanisms," *Journal of Dynamic Systems, Measurements and Control,* Vol. 104, No. 3, 1982, pp. 205–211.

[22]Strang, G., *Introduction to Applied Mathematics,* Wellesley-Cambridge, Wellesley, MA, 1986, pp. 1–61.